https://doi.org/10.5194/egusphere-2022-908
Preprint. Discussion started: 5 October 2022

Abrasion of sedimentary rocks as a source of hydrogen peroxide and nutrients to subglacial ecosystems

Beatriz Gill-Olivas[1], Jon Telling[2], Mark Skidmore[3], Martyn Tranter[1]

[1] Department of Environmental Science, Aarhus University, Roskilde, Denmark.
[2] School of Natural and Environmental Sciences, Newcastle University, Newcastle, UK.
[3] Department of Earth Sciences, Montana State University, Bozeman, United States.

Correspondence to: Beatriz Gill-Olivas (b.gillolivas@envs.au.dk)

Abstract. Glaciers and ice-sheets are renowned for their abrasive power, yet little is known of the mechanochemical reactions which are initiated by abrasion in these environments and their effect on subglacial biogeochemistry. Here, we use sedimentary rocks representative of different subglacial environments and from a previously glaciated terrain to investigate the potential for subglacial erosion to generate H_2O_2 and release bio-utilisable organic carbon and nutrients (N, Fe). Samples were crushed using a ball mill, water added to rock powders within gastight vials, and samples incubated in the dark at 4°C. Headspace and water samples were taken immediately after the addition of water and then again after 5 and 25 h. Samples generated up to 1.5 µmol H_2O_2 g^{-1}. The total sulphur content, a proxy for the sulphide content, did not correlate with H_2O_2 generation, suggesting that the pyrite content was not the sole determinant of net H_2O_2 production. Other factors, including the presence of carbonates, Fe-driven Fenton reactions and the pH of the solution were also likely to be important in controlling both the initial rate of production and subsequent rates of destruction of H_2O_2. Further, we found erosion can provide previously unaccounted sources of bio-utilisable energy substrates and nutrients, including up to 880 nmol CH_4 g^{-1}, 680 nmol H_2 g^{-1}, volatile fatty acids (up to 1.7 µmol acetate g^{-1}) and 8.2 µmol NH_4^+ g^{-1} to subglacial ecosystems. These results highlight the potentially important role that abrasion plays in providing nutrient and energy sources to subglacial microbial ecosystems underlain by sedimentary rocks.

1 Introduction

The link between physical erosion and the products of chemical weathering has long been established (Anderson, 2005). However, only a few studies have attempted to understand the chemical reactions triggered explicitly by mechanical abrasion within these environments. These have primarily focused on the potential reactivity of silicates after comminution (Gill-Olivas et al., 2021; Telling et al., 2015) and the release or production of gases during comminution (Gill-Olivas et al., 2021; Macdonald et al., 2018). It has been shown that comminution of certain rocks and minerals can generate strong redox agents, such as H_2 (Saruwatari et al., 2004; Takehiro et al., 2011; Telling et al., 2015; Wakita et al., 1980; Edgar et al., 2022) and H_2O_2 (Bak et al., 2017; Borda et al., 2003; He et al., 2021; Edgar et al., 2022; Stone et al., 2022). These are expected to have an

https://doi.org/10.5194/egusphere-2022-908
Preprint. Discussion started: 5 October 2022

influence on the wider hydrochemistry of subglacial systems, particularly as biogeochemical reactions in these environments rely heavily on redox gradients (Tranter et al., 2005).

To date, studies of subglacial biogeochemistry have largely focused on both abiotic and biotically mediated weathering reactions (Hodson et al., 2008; Tranter et al., 2002b; Skidmore et al., 2010). Subglacial environments are often dominated by the comminution products of silicate and/or siliciclastic rocks (Wadham et al., 2010; Hodson et al., 2000). Nevertheless, it was thought until recently that their effect on the hydrochemistry of glacier systems was minimised by their slow dissolution kinetics (Lerman, 1988), with significant quantities of solute derived from silicate weathering only being associated with larger ice-sheets, where there is a longer subglacial water residence time (Wadham et al., 2010). In contrast, carbonate weathering, which has more rapid dissolution kinetics, is thought to dominate the subglacial hydrochemistry even when only present in trace quantities in the comminuted bedrock (Tranter et al., 1993). This is particularly true of smaller catchment glaciers (Wadham et al., 2010). Nevertheless, carbonate weathering is partly constrained by the availability of protons (H^+; Eq. (R1); Plummer et al. (1978)). H^+ can be derived from carbon dioxide (CO_2) dissolving in water and generating carbonic acid (H_2CO_3; Eq. (R2); Plummer et al. (1978)). In subglacial systems, where atmospheric CO_2 is limited, Eq. (R1) and (R2) are partly regulated by CO_2 generated from organic matter oxidation (Tranter et al., 2002a). Weathering may become dominated by carbonate hydrolysis in the absence of other proton sources,, which does not require a source of H^+ or CO_2 (Eq. (R3); Plummer et al. (1978)).

$$CaCO_3\,(s) + H^+(aq) \leftrightarrows Ca^{2+}\,(aq) + HCO_3^-\,(aq) \quad \text{(R1)}$$

$$CaCO_3\,(s) + H_2CO_3^0\,(aq) \leftrightarrows Ca^{2+}\,(aq) + 2HCO_3^-\,(aq) \quad \text{(R2)}$$

$$CaCO_3\,(s) + H_2O\,(l) \leftrightarrows Ca^{2+}(aq) + HCO_3^-\,(aq) + OH^-\,(aq) \quad \text{(R3)}$$

Sulphide (most commonly, FeS_2) oxidation is often a source of H^+ in subglacial environments (Montross et al., 2013b). Sulphide oxidation can be coupled to both carbonate and silicate hydrolysis (Tranter, 2003) (Eq. (R4) and (R5), respectively).

$$4FeS_2(s) + 16Ca_{1-x}(Mg_x)CO_3(s) + 15O_2(aq) + 14H_2O(l) \leftrightarrows 16(1-x)Ca^{2+}(aq) + 16xMg^{2+}(aq) + 16HCO_3^-\,(aq) + 8SO_4^{2-}(aq) + 4Fe(OH)_3(s) \quad \text{(R4)}$$

$$4FeS_2(s) + 16Na_{1-x}K_xAlSi_3O_8(s) + 15O_2(aq) + 86H_2O(l) \leftrightarrows 16(1-x)Na^+(aq) + 16xK^+(aq) + 8SO_4^{2-}(aq) + 4Al_4Si_4O_{10}(OH)_8\,(s) + 32H_4SiO_4\,(aq) + 4Fe(OH)_3\,(s) \quad \text{(R5)}$$

These reactions occur when glacial flour, crushed bedrock, comes into contact with water at the glacier bed. It is often the case that trace quantities of sulphides and carbonates are liberated from the matrix of silicate minerals by crushing, but there are other effects of physical abrasion or comminution on subglacial biogeochemistry, our knowledge of which, are still in its infancy. The potential solute contribution from abraded sediments of Subglacial Lake Whillans (SLW), West Antarctica, was briefly discussed in Gill-Olivas et al. (2021). These heavily weathered sediments released significant concentrations of biologically relevant solutes, such as ammonium (NH_4^+) and acetate (CH_3COO^-), as well as other major ions, most likely from

https://doi.org/10.5194/egusphere-2022-908
Preprint. Discussion started: 5 October 2022

fluid inclusions, following comminution (Gill-Olivas et al., 2021). The erosion of silicate minerals under subglacial conditions has been shown to produce hydrogen (H_2) through mechanochemical reactions (Eq. R6 – R8; Kita et al. (1982)). The solubility of H_2 in water increases at low temperatures and high pressures (Wiebe and Gaddy, 1934). This makes mechanochemical reactions a potentially significant source of H_2 for microbial processes including methanogenesis in subglacial waters (Gill-Olivas et al., 2021; Telling et al., 2015; Dunham et al., 2021). Abrasion of minerals can also generate protons through the generation and dissolution of CO_2 (Macdonald et al., 2018) or through the heterolytic cleavage of Si-O bonds (Eq. (R9); Stillings et al. (2021)), further lowering the saturation index with respect to carbonates.

$$\equiv Si - O - Si \equiv \longrightarrow \equiv Si\cdot + \cdot O - Si \equiv \quad \text{(R6)}$$

$$\equiv Si\cdot + H_2O \rightarrow SiOH + H\cdot \quad \text{(R7)}$$

$$H\cdot + H\cdot \rightarrow H_2 \quad \text{(R8)}$$

$$\equiv Si^+ + H_2O \rightarrow SiOH + H^+ \quad \text{(R9)}$$

Abrasion of FeS_2 can also trigger chemical reactions, including Fenton reactions (Gil-Lozano et al., 2017). Crushing, breaks S-S bonds in FeS_2, generating dangling S^- sites (Nesbitt et al., 1998). These S^- sites are then stabilised by acquiring an electron from the adjoining Fe^{2+} ions, thus producing surface Fe^{3+} and S^{2-} (Eq. (R10)). Water is split by the surface Fe^{3+} to produce ·OH (Eq. (R11); Borda et al. (2003)). Thereafter, two ·OH can react together to produce H_2O_2 (Eq. (R12); Borda et al. (2001)). There are multiple sources and sinks for surface and free radicals in natural systems (Gill-Olivas et al., 2021), and there is currently a need to address how the complex mineralogy of natural rock and sediment samples may hinder or enhance the relative magnitudes of these reactions.

$$Fe^{2+}_{surface} + S^{-}_{surface} \rightarrow Fe^{3+}_{surface} + S^{2-}_{surface} \quad \text{(R10)}$$

$$Fe^{3+}_{surface} + H_2O_{(ads)} \rightarrow Fe^{2+}_{surface} + \cdot OH_{(ads)} + H^+ \quad \text{(R11)}$$

$$\cdot OH + \cdot OH \rightarrow H_2O_2 \quad \text{(R12)}$$

The production of H_2O_2 by comminution may have significant consequences for the organic matter (OM) found in these environments. Subglacial environments are largely isolated from external OM inputs, but as certain glaciers form, they may override and incorporate pre-existing soil (Kohler et al., 2017), vegetation (Souchez et al., 2006) and/or lake and marine sediments (Michaud et al., 2016), thus integrating any associated OM into subglacial sediments (Wadham et al., 2019). This overridden OM can fuel microbial activity to produce CO_2 or CH_4 (Stibal et al., 2012). These gases are then either utilised by further microbial activity (Michaud et al., 2017), transported within the hydrological system or, in the case of CH_4, may be stored as gas hydrates (Wadham et al., 2019). Additionally, OM contains organic acids which can act as an additional proton source for subglacial weathering (Montross et al., 2013b). Hydrogen peroxide is a strong oxidising agent which can oxidise OM to CO_2. Thus, H_2O_2 production via erosion of these sediments could be problematic to microbial ecosystems, if the

https://doi.org/10.5194/egusphere-2022-908
Preprint. Discussion started: 5 October 2022

concentration of H_2O_2 exceeds 0.08% ((Medina-Cordoba et al., 2018)). However, it has been suggested that H_2O_2 might serve to oxidise and reactivate otherwise refractive organic molecules in subglacial systems (Tranter, 2015). A number of studies have concluded that DOC and POC exported from glacial systems is highly bio-available (Lawson et al., 2014), yet is also paradoxically ancient (Hood et al., 2009), lending some credence to the potential re-activation of ancient OM through erosion (Tranter, 2015).

Here, we aim to further understand the generation of H_2O_2 by the comminution of various pyrite-containing sedimentary rocks and subglacial sediments. We hypothesise that the concentration of sulphide in sedimentary rocks would have a first order impact on the amount of H_2O_2 that is generated when the rocks are crushed. Further, we aim to investigate how the generation of H_2O_2 may affect the availability of OM present in these rocks and the potential release of bio-available compounds. We do this by investigating the H_2O_2 generation, the overall water chemistry and the release of gases when three different shale sedimentary rocks, shale, siltstone and muddy carbonate samples and one subglacial sediment sample, chosen for their varying C, OC and S contents (Table 1), were crushed.

Table 1 Total concentration of N, Inorganic Carbon (IC), Organic Carbon (OC), and S, as determined by Elemental Analysis, and specific surface area (SSA) of samples.

Sample name		%N	%IC	%OC	%S	SSA (m^2/g)
Svalbard Siltstone (SSv)	**- Coarse**	0.7	0.6	26.2	**0.2**	0.84
	- Crushed	0.7	0.6	26.2	**0.2**	6.51
Jurassic Shale (JS)	**- Coarse**	0.2	0.9	4.2	**0.4**	22.7
	- Crushed	0.2	0.9	4.2	**0.4**	40.3
Robertson Muddy Carbonate (RMC)	**- Coarse**	0.1	6.3	1.1	**0.3**	4.71
	- Crushed	0.1	6.3	1.1	**0.3**	40.9
Mercer Subglacial Lake (SLM)	**- Coarse**	0.02	0.2	0.1	**0.02**	17.9
	- Crushed	0.02	0.2	0.1	**0.02**	15.4

Methodology

2.1 Sample Sites

A selection of rocks and a sediment sample spanning a range of carbon (C), nitrogen (N), sulphur (S), and organic carbon (OC) from three different glaciated catchments and a rock sampled from a previously glaciated terrain were utilised in this study.

https://doi.org/10.5194/egusphere-2022-908
Preprint. Discussion started: 5 October 2022

Jurassic Shale (JS) from Yorkshire (UK), purchased from Northern Geological Supplies Ltd., was used as a positive control for these experiments due to its relatively high pyrite content (Table 1). Further, these rocks were likely overlain by ice during the last glacial maximum. Samples from glaciated environments included rock samples collected near Longyearbreen (SSv; Svalbard 78.1941° N, 15.5475° W) and Robertson Glacier (RMC; Canadian Rockies 50.738200° N, 115.331734° W), and a subglacial sediment sample from Mercer Subglacial Lake (SLM; Antarctica, (84.640287° S, 149.501340° W). The bedrock underlaying Longyearbyen and surrounding areas are primarily from the Early Cretaceous Epoch (Helvetiafjell and Carolinefjell formation) and from the late Paleocene to Early Eocene Epoch (Firkanten, Basilika and Battfjellet Formations) and consist primarily of sedimentary rocks including sandstones, siltstones, mudstones and shales (Elvevold et al., 2007). The local bedrock underlying Robertson Glacier is Upper Devonian in age (Mount Hawk, Palliser, and Sassenach Formations) and consists of impure limestones, dolostones, and dolomitic limestones, with interbeds of shale, siltstone, and sandstone (Mcmechan, 1998). The sample from SLM, was material from the core catcher from a 1.76 m long core (SLM1801-02FF-2) (Priscu et al., 2021). The basal sediments from the core were clast-rich massive, muddy glacial diamict (Campbell et al., 2019), similar in composition to the diamicts from beneath the neighboring Whillans Ice Stream (Tulaczyk et al., 1998) and Subglacial Lake Whillans (SLW) (Hodson et al., 2016). The matrix supported diamict was very poorly sorted (Folk and Ward, 1957) with the matrix composed of predominantly silt (52%), with contributions of sand (25%) and clay (23%) (Campbell et al., 2019).

2.2 Elemental Analysis

C, N and S concentrations in the samples were determined using an elemental analyser (Elementar Vario PYRO Cube, Langenselbold, Hesse, DE). Triplicate 5 mg to 20 mg of crushed samples were weighed into tin capsules and introduced into the machine. The organic carbon (OC) concentrations was determined following techniques in Harris et al. (2001). Some 20 mg to 30 mg of crushed samples were weighed into silver capsules (part num.: S05003397). The capsules were transferred to a microtiter plate, and wetted with 50 µL of 18.2 MΩ water, then transferred to a desiccator. A beaker with ~100 ml 12 M HCl was also placed inside this desiccator and the samples were exposed to the HCl vapours overnight (~14 h), then dried in an oven at 60 °C for 4 h, then placed within another silver capsule and closed. These fumigated samples were then introduced into the elemental analyser (Elementar Vario PYRO Cube, Langenselbold, Hesse, DE) as before. The detection limit was 0.001% for all three elements and the coefficient of variation (CV) for C, N and S for eight replicates of a soil analytical standard (NCS Soil Standard 338 40025, cert. 133317, C = 2.29%, N = 0.21%, S = 0.031%; Elemental Microanalysis Ltd., United Kingdom) were 4.9%, 5.3% and 18%, respectively.

2.3 Sample Preparation and Dry Crushing

The rock samples were washed with 18.2 MΩ cm^{-1} water and dried at 75 °C for over 18 hours (after which there was no mass change). RMC and JS samples were then wrapped in several layers of paper roll bags (to avoid metal–rock interaction) and

https://doi.org/10.5194/egusphere-2022-908
Preprint. Discussion started: 5 October 2022

broken using sledgehammer on a metal plate. SSv was broken using an agate pestle and mortar, and SLM sediments disaggregated also using an agate pestle and mortar. The broken rocks and sediment were sieved and the 125 µm to 2 mm size fraction was collected (hereafter referred to as the 'Coarse' samples). The 'Crushed' samples were prepared by crushing 15 g of the coarse samples in air for 30 minutes within a zirconium oxide ball mill at 500 r.p.m using a Fritsch Planetary Mono Mill Pulverisette 6 (FRITSCH GmbH, Idar-Oberstein, Germany).

2.4 Microcosm Experiments

Triplicate 1 g coarse samples for each timepoint, were weighed into 50 mL borosilicate serum vials (Wheaton ®, VWR), which had been previously acid washed, rinsed six times with 18.2 MΩ cm^{-1} water and furnaced at 450 °C for 4 hours. These vials were then sealed with grey butyl rubber stoppers, which had been previously washed in 3% Decon® 90, acid washed, soaked in 18.2 MΩ water overnight before rinsing six times with 18.2 MΩ cm^{-1} water. The same procedure was followed for crushed samples immediately after milling. Three borosilicate vials were sealed without the addition of samples for use as rock free controls (blanks) at each timepoint. Then, 15 mL aliquots of 18.2 MΩ cm^{-1} water, which had been pre-autoclaved and cooled to 4 °C, were added to each vial in turn. The vials were shaken by hand to mix, and a 10 mL headspace gas sample was taken by over pressurizing the vials with 10 mL of N_2 and transferring the gas into a 5.9 mL Exetainer® (Labco, Lampeter, UK). Next, the serum vials were opened, and the slurry was filtered using a 0.22 µm PES Steriflip® Vacuum Filtration System (Millipore). A 4 mL filtrate aliquot was taken to analyse pH (using Hach® Sension+ 5208), followed by analysis of H_2O_2 concentration. The same procedure was followed for samples taken 5 and 25 hours after the addition of water.

2.5 Hydrogen Peroxide Analysis

A 4 mL aliquot of the filtered solution was used for H_2O_2 analysis using neocuprine (2,9-Dimethyl-1,10-phenanthroline (Product #: N1501; Sigma-Aldrich), based on the methods in Baga et al. (1988) and Borda et al. (2001). Standards (0 to 100 µM) were prepared using known concentrations of H_2O_2 (ESMURE® ISO, 30% Hydrogen Peroxide, Perhydrol®, Millipore). 4 mL of each standard was pipetted into a 15 mL centrifuge tube, and to this, 1 mL of 0.01 M Copper (II) Sulphate, and 1 mL of neocuprine solution (10 g L^{-1} in ethanol) were added. The solution was then made up to 10 mL with 18.2 MΩ water and the absorbance of the solution was measured at 454 nm using a Shimadzu UV mini 1240 UV-VIS spectrophotometer (Shimadzu, Kyoto, Japan).

2.6 Gas Analysis

Headspace gas samples were taken from the ball mill before and after crushing by over pressurizing the ball mill with 10 mL of oxygen-free N_2 (zero grade, BOC). Then, a 10 mL headspace gas aliquot was transferred into a 5.9 mL pre-evacuated double-waded Exetainer® (Labco, Lampeter, UK) using a gas-tight syringe. Headspace gases from the vials were sampled immediately after the addition of water and after 5 and 25 hours. The contents of the Exetainers® were then analysed using an Agilent 8860 Gas Chromatograph (Agilent Technologies, Santa Clara, CA, USA). Concentrations of CH_4 and CO_2 were

https://doi.org/10.5194/egusphere-2022-908
Preprint. Discussion started: 5 October 2022

determined by a Flame Ionization Detector (FID). The sample loop was 0.5 mL, Helium (He) was used as the carrier gas, and a Porapak Q 80-100 mesh, 2 m × 1/8 inch × 2 mm SS column and a methaniser were used to distinguish the compounds. The concentrations of H_2 and O_2 were determined using a Thermal Conductivity Detector (TCD), using a 1 mL sample loop, Argon (Ar) as the carrier gas, and a Hayesep D 80–100 mesh, 2 m × 1/8 inch SS column, in series with a molecular sieve 5a, 60–80 mesh, 8 ft × 1/8 inch column. The oven temperature was set at 30°C for the initial 4 mins, and then the temperature ramped up at rate of 50 °C min^{-1} until the oven reached a temperature of 200 °C. This temperature was maintained for 2.5 mins, when the run was concluded. The concentrations of headspace gases were calculated based on a standard-curve generated from the dilution of an 11 mixed gas standard (173738-AH-C, BOC). The standard-curve was linear over the concentration ranges for H_2: 4.1 ppm to 502 ppm, R^2 = 0.9988, n = 6; for CH_4: 1.6 ppm to 198 ppm, R^2 = 0.9988, n = 7; for CO_2: 3.4 ppm to 398 ppm, R^2 = 0.9992, n = 7. Standards were run daily and gave a CV of 1.2% (n = 31) for H_2, with a detection limit of 2.2 ppm, equivalent to 5.2 nmol g^{-1}, a CV of 1.2% (n = 31) for CH_4, with a detection limit of 0.11 ppm, equivalent to 0.26 nmol g^{-1} and a CV of 4.3% (n = 31) for CO_2, with a detection limit of 0.40 ppm, equivalent to 0.93 nmol g^{-1}. The ideal gas law was used to convert to molar concentrations, and concentrations were corrected for dilution during sampling and for gases dissolved in the water using Henry's diffusion coefficient (where relevant). The results were also blank corrected and normalised to dry sediment mass.

2.7 Water Chemistry Analysis

Anions and organic acids, including: acetate (Limit of detection (LOD): 0.052 ppm, equivalent to 0.14 µmol g^{-1}; CV: 0.76%), formate (LOD: 0.018 ppm, equivalent to 0.06 µmol g^{-1}; CV: 1.07%), SO_4^{2-} (LOD: 0.22 ppm, equivalent to 0.37 µmol g^{-1}; CV: 1.41%), and oxalate (LOD: 0.020 ppm, equivalent to 0.04 µmol g^{-1}; CV: 0.48%) were analysed using a Dionex ICS 6000 (ThermoScientific), fitted with a Dionex IonPac™ AS11-HC 4 µm column.

Additional aliquots of the filtered solution were subsampled to analyse for NH_4^+ (LOD: 0.026 ppm, equivalent to 0.3 µmol g^{-1}; CV: 2.3%), and total Fe (LOD: 0.17 ppm, equivalent to 0.5 nmol g^{-1}; CV: 1.5%) using the Gallery Automated Photometric Analyzer (Thermofisher). For NH_4^+ analysis, aliquots of JS and SLM were diluted 1 in 10, and aliquots of SSv and RMC were diluted 1 in 20 (due to their concentration being greater than the highest standard). Concentrations of NH_4^+ were then determined using an adapted version of the salicylate method outlined in Le and Boyd (2012). The concentration of total Fe was determined using an adapted version of the ferrozine method described in Viollier et al. (2000), using undiluted aliquots of the filtered solution.

2.8 Specific Surface Area

The specific surface area (SSA) of materials was measured using a NOVA 1200e BET Analysis System. Approximately 1 g of dried sample was loaded into a pre-calibrated sample cell. The whole system was then evacuated and dried at 110 °C for a

https://doi.org/10.5194/egusphere-2022-908
Preprint. Discussion started: 5 October 2022

minimum of six hours (Zhou et al., 2019). The surface area of materials was measured using nitrogen gas as an adsorbent at 77 K.

3 Results

3.1 Hydrogen Peroxide

Overall, crushed samples produced more H_2O_2 than their coarse counterparts, and the concentration increased over the first 25 hours. SSv samples produced the highest concentration of H_2O_2, with crushed samples producing up to 1.5 µmol H_2O_2 g^{-1} (Fig. 1a), and coarse samples producing up to 1.3 µmol H_2O_2 g^{-1} (Fig. 1a). The concentration of H_2O_2 in SSv increased between the 5 min and 5 hour time points, but then decreased at the 25 hour time point, in contrast with the continual rise in concentration shown by the other samples. The crushed RMC and JS samples, which also produced quantifiable H_2O_2 concentrations, generated an order of magnitude less H_2O_2 than crushed SSv samples, with maximum concentrations of 0.23 and 0.20 µmol g^{-1} respectively (Fig. 1b). The concentration of H_2O_2 produced by coarse JS samples was only slightly lower than that of its crushed counterpart (maximum of 0.12 µmol g^{-1}, Fig. 1b). The concentration produced by coarse RMC was considerably lower than its crushed equivalent, reaching a maximum of 0.02 µmol g^{-1} (Fig. 1b). SLM samples barely produced any H_2O_2 above the LOD; only after 25 hours was the concentration of H_2O_2 in crushed samples quantifiable (maximum value of 0.03 µmol g^{-1}; Fig. 1b). This contrasts with the concentrations of H_2O_2 produced by crushed Subglacial Lake Whillans samples, which were much higher (up to 17 µmol g^{-1}; Gill-Olivas et al. (2021)).

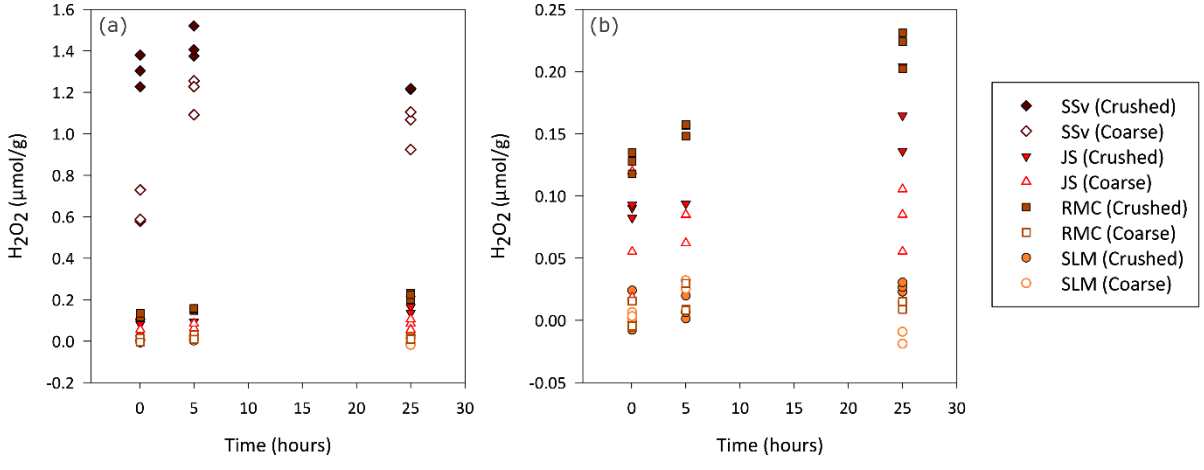

Figure 1 Concentration of H_2O_2 generated by coarse and crushed samples. (a) Blank corrected H_2O_2 µmol produced per gram of crushed and coarse sediment samples. (b) Focus on lower concentrations of H_2O_2, excluding results of coarse and crushed SSv samples, to allow a clearer view of the data distribution of the remaining samples.

https://doi.org/10.5194/egusphere-2022-908
Preprint. Discussion started: 5 October 2022

Production of H_2O_2 was weakly correlated to the concentration of SO_4^{2-} in the solution in samples with low H_2O_2 (R^2 = 0.432; Fig. 2a) and more strongly correlated with the SSA of these samples (R^2 = 0.706; Fig. 2c). The concentration of H_2O_2 produced by SSv did not fall on these regression lines. The production of H_2O_2 from SSv samples shows a weak correlation with SO_4^{2-} and SSA (R^2= 0.530, Fig. 2a; R^2= 0.484, Fig. 2c), however, this is a limited sample size so care should be taken in interpreting these correlations. Total dissolved Fe was only detected in SSv samples, and this also showed a weak correlation with H_2O_2 concentrations (R^2= 0.493, Fig. 2b).

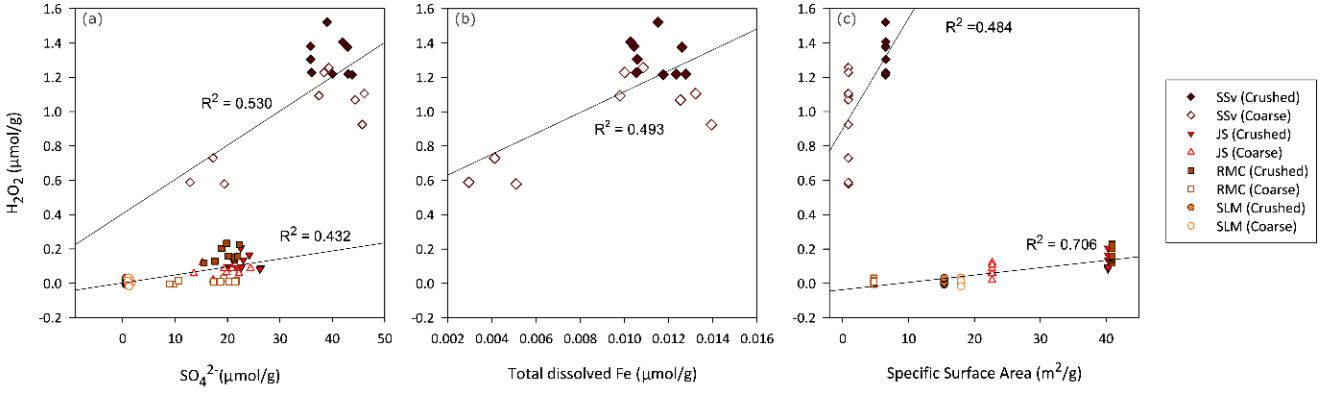

Figure 2 Relationships between concentration of H2O2 (µmol) produced per gram of crushed and coarse samples relative to (a) sulphate, (b) iron and (c) specific surface area. The concentrations of sulphate (a) and dissolved Fe (b) measured in solution are normalised to gram of sample. Note Fe concentrations were above detection limits only in the SSv samples.

3.2 Ammonium in Solution

All crushed samples produced significantly higher concentrations of NH_4^+ in solution compared to their coarse counterparts (Wilcox test, $p \leq 0.01$; Fig. 3a). There was no clear temporal trend to the production of NH_4^+, other than potentially a slight increase with time for RMC samples (Fig. 3b). After 25 hours, crushed RMC samples showed the highest NH_4^+ concentrations (up to 8.2 µmol g^{-1}), closely followed by crushed JS samples (up to 6.6 µmol g^{-1}). This is considerably higher than their coarse counterparts with concentrations of up to 0.20 and 0.99 µmol g^{-1}, for RMC and JS samples respectively (Fig. 3a).

https://doi.org/10.5194/egusphere-2022-908
Preprint. Discussion started: 5 October 2022

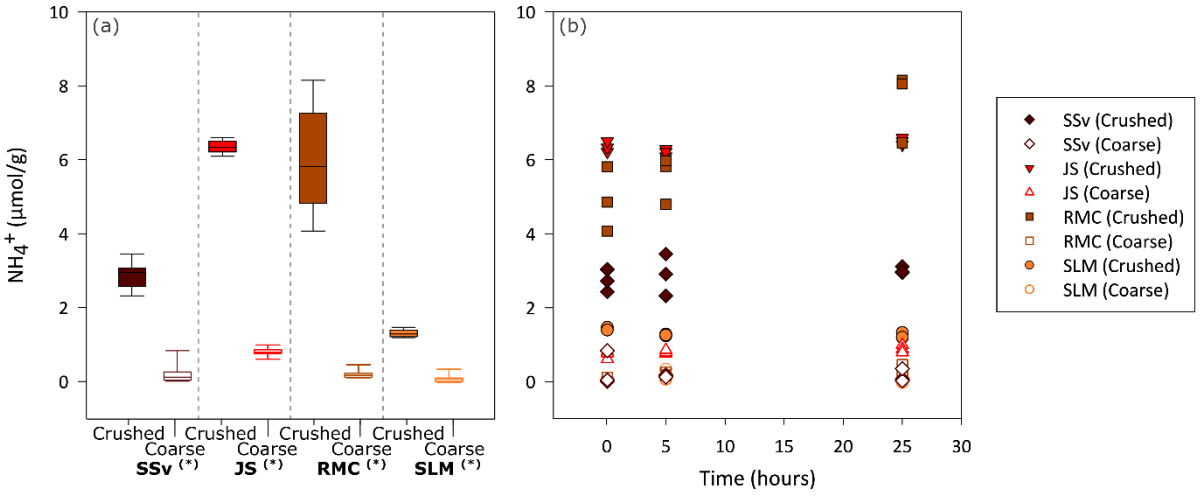

Figure 3 Concentration of NH4+ in solution. (a) Boxplot showing the range of NH4+ measured in solution (normalised to µmol NH4+ g-1) for all time points in the incubation of coarse and crushed samples (n = 9 for each sample type). Highly significant difference ($p \leq 0.01$) between crushed and coarse samples is denoted by (*). The minimum and maximum values are represented by the whiskers, the interquartile range is represented by the box, and the median value is shown by the line in the centre of the box (b) Concentration of NH4+ in solution (normalised to µmol NH4+ g-1) after approximately 5 minutes, and 5 and 25 h of incubation.

3.3 Organic Acids

All crushed and coarse samples produced quantifiable concentrations of acetate (Fig. 4a), and, in some cases, formate (Fig. 4b). There was a significant range of values for acetate concentrations and no clear temporal trend throughout the 25 hour incubations. However, SSv and JS samples showed a highly significant (Wilcox test, $p \leq 0.01$) and significant (Wilcox test, $p \leq 0.05$) difference between crushed and coarse samples (Fig. 4a). Formate concentrations were lower, than acetate but all samples, except for RMC, showed a highly significant difference between crushed and coarse samples (Wilcox test, $p \leq 0.01$). JS produced the highest concentrations of both acetate (median of 1.7 µmol g^{-1} for crushed samples; Fig. 4a) and formate (median of 0.38 µmol g^{-1} crushed samples; Fig. 4b). SLM and SSv both produced considerably less acetate (median of 0.11 and 0.21 µmol g^{-1} for crushed samples respectively; Fig. 4a). Formate concentrations were also low in SSv samples, SLM samples produced slightly more formate (median of 0.03 and 0.11 µmol g^{-1} respectively, Fig. 4b). RMC samples showed considerable variability in acetate concentrations and little if any formate.

https://doi.org/10.5194/egusphere-2022-908
Preprint. Discussion started: 5 October 2022

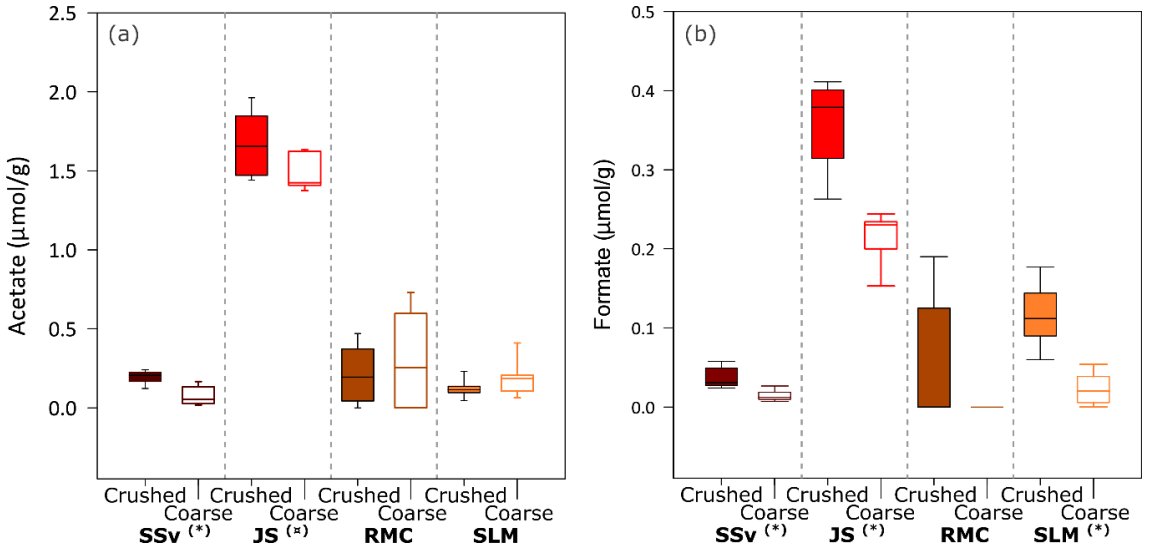

Figure 4 Concentration of acetate and formate in solution at all incubation timepoints. Boxplots of (a) acetate concentration in solution (normalised to µmol acetate g-1) and (b) formate concentration in solution (normalised to µmol formate g-1) after the incubation of coarse and crushed samples (n = 9, for each sample type). Highly significant difference (p ≤ 0.01) between crushed and coarse samples is denoted by (*). Significant difference (p ≤ 0.05) between crushed and coarse samples is denoted by (¤). The minimum and maximum values are represented by the whiskers, the interquartile range is represented by the box, and the median value is shown by the line in the centre of the box.

3.4 pH

Overall, the pH of all samples stayed relatively stable over the incubation time of 25 hours. Crushed samples appeared to have slightly higher pH than their coarse counterparts, potentially due to the release of calcite leading to carbonate reactions, elevating the pH (Fig. 5). Most samples had pH close to neutral or above, the only exception was SSv incubations which were acidic, with an median pH of 3.61 and 3.11 in crushed and coarse samples, respectively (Fig. 5).

3.5 Gases Released

All rock samples produced quantifiable concentrations of CH_4, CO_2 and H_2 gas above atmospheric concentrations (Table 2). RMC produced the highest concentrations of CH_4 and CO_2 (880 nmol CH_4 g^{-1} and 2800 nmol CO_2 g^{-1}; Table 2) during crushing, and produced quantifiable C_2H_6 concentrations (3.5 nmol g^{-1}; Table 2). JS samples produced noticeable concentrations of CH_4 and CO_2 as well C_2H_6 (47, 1100 and 4.5 nmol g^{-1}, respectively; Table 2). JS samples also produced the highest H_2 concentrations measured (680 nmol g^{-1}; Table 2). SSv produced less CH_4, CO_2, C_2H_6 and H_2 than JS and RMC samples and SLM produced the lowest concentration of CH_4 out of these samples (7.2 nmol g^{-1}; Table 2) and no CO_2 and C_2H_6 above the LOD. However, they did release significant concentrations of H_2 during crushing (220 nmol g^{-1}, Table 2).

https://doi.org/10.5194/egusphere-2022-908
Preprint. Discussion started: 5 October 2022

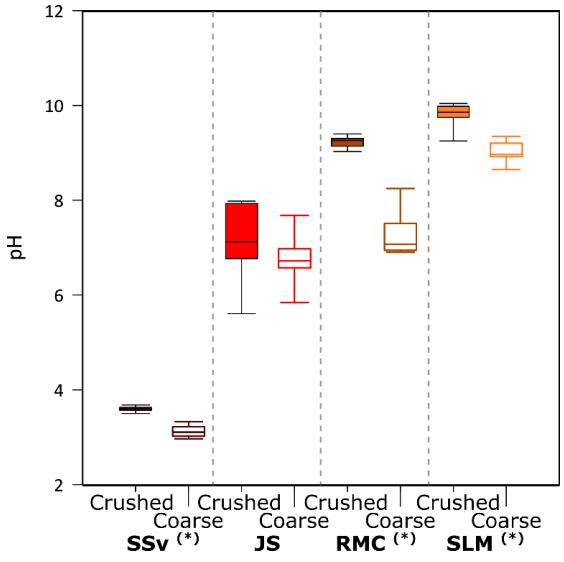

Figure 5 pH of solutions at all incubation time points with crushed and coarse samples. (n = 9 for each rock type and treatment). Highly significant difference ($p \leq 0.01$) between crushed and coarse samples is denoted by (*). The minimum and maximum values are represented by the whiskers, the interquartile range is represented by the box, and the median value is shown by the line in the centre of the box.

Table 2 Gases released to ball mill headspace during high energy crushing of samples. Values were corrected for initial atmospheric gas concentrations.

		nmol Gas produced /g during initial crushing			
		CH_4	CO_2	C_2H_6	H_2
Svalbard Siltstone (SSv)	**- Coarse**	-	-	-	-
	- Crushed	26.8	140	0.0	41.1
Jurassic Shale (JS)	**- Coarse**	-	-	-	-
	- Crushed	47.2	1076	4.5	683
Robertson Muddy Carbonate (RMC)	**- Coarse**	-	-	-	-
	- Crushed	882	2790	3.5	98.6
Subglacial Lake Mercer (SLM)	**- Coarse**	-	-	-	-
	- Crushed	7.2	-59.1	0.0	218

https://doi.org/10.5194/egusphere-2022-908
Preprint. Discussion started: 5 October 2022

During incubations, the concentrations of the gases CO_2, H_2 and C_2H_6 were, for the most part, indistinguishable from the noise in the analysis of these gas concentration in laboratory air. However, crushed RMC samples did produce CH_4 concentrations over the 25 hour incubation which could be quantified, increasing from an average of 20 to 64 nmol g^{-1} (Fig. 6). JS crushed samples also produced quantifiable CH_4, although at much lower concentrations, below LOD at 5 min and an average of 1.1 and 1.3 nmol g^{-1} after 5 and 25 hours, respectively (Fig. 6).

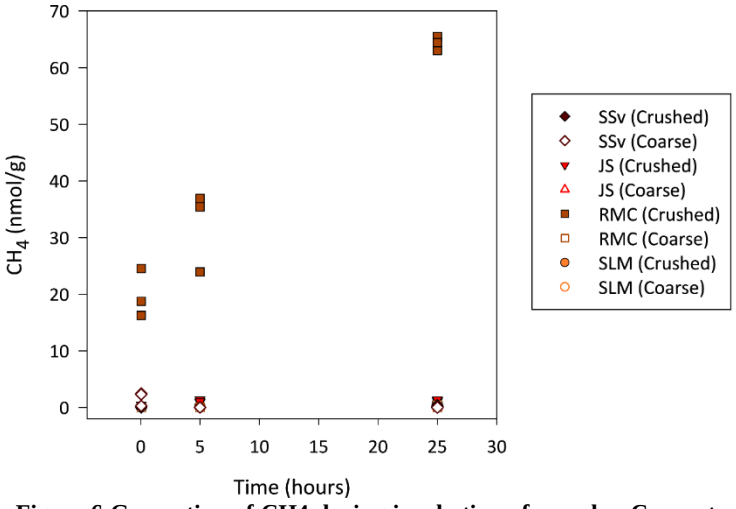

Figure 6 Generation of CH4 during incubation of samples. Concentration of CH4 in headspace gases during incubation of coarse and crushed samples, blank corrected and normalised to the grams of sample.

4 Discussion

4.1 The effect of mineralogy on oxidant production

The concentration of S in the samples (Table 1) was assumed to be indicative of pyrite content, since no other sulphur containing minerals (e.g. anhydrite, gypsum) have been reported for the rocks/sediments (Mcmechan, 1998; Campbell et al., 2019; Elvevold et al., 2007). Thus, it was expected that samples with higher S content would also produce more H_2O_2 when crushed, if crushed samples had similar surface areas. However, our results showed SSv samples produced considerably more H_2O_2 (Fig. 1a) than other rock samples, despite the relatively low S content and SSA (Table 1), indicating other factors played a role in the generation and/or consumption of H_2O_2. We focus on generation first.

The rupture of Fe-S and S-S bonds in pyrite has been shown to produce H_2O_2 in both oxic (Nesbitt et al., 1998) and anoxic conditions (Eq. (R10) - (R12); Borda et al. (2003)). Simultaneously, the release of Fe^{2+} into solution due to dissolution of FeS_2 can catalyse the Fenton and Haber-Weisse reaction, removing H_2O_2 and generating other reactive oxygen species (ROS) (Eq. (R13) – (R16); Gil-Lozano et al. (2017)). Hydroxyl radicals (·OH) are often suggested as an intermediate, which can react together to regenerate H_2O_2 (Eq. (R17)). However, this only occurs under acidic conditions (Bataineh et al., 2012). Solutions

https://doi.org/10.5194/egusphere-2022-908
Preprint. Discussion started: 5 October 2022

from SSv samples had an acidic pH (Fig. 5), and so these samples may have generated more ·OH, and thus sustain H_2O_2 concentrations generated by crushing (Fig. 1a).

$$H_2O_2 + Fe^{2+} \rightarrow Fe^{3+} + OH^- + \cdot OH \quad \text{(R13)}$$

$$H_2O_2 + Fe^{3+} \rightarrow Fe^{2+} + H^+ + \cdot O_2H \quad \text{(R14)}$$

$$\cdot O_2H \rightarrow O_2^- \cdot + H^+ \quad \text{(R15)}$$

$$O_2^- \cdot + H_2O_2 \rightarrow \cdot OH + O_2 + OH^- \quad \text{(R16)}$$

$$\cdot OH + \cdot OH \rightarrow H_2O_2 \quad \text{(R17)}$$

Fe(IV) is preferentially produced as a Fenton intermediate at circumneutral pH (Bataineh et al., 2012), thus rapidly utilising any H_2O_2 produced from abrasion of pyrite. Further, studies into the Fenton reaction in biological systems suggest that where HCO_3^- is present, carbonate-radical-anions ($CO_3\cdot^-$) will be the most likely product of the Fenton reaction (Illes et al., 2019). Solutions incubated with JS and RMC samples had a circumneutral to basic pH (Fig. 5), and the rocks had relatively high carbonate contents (Table 1). Therefore, it is likely that $CO_3\cdot^-$ was produced as a Fenton product despite the higher pyrite content in these samples, so yielding less H_2O_2. The SLM samples produced limited H_2O_2, (Fig. 1a), despite the lower carbonate content of the sediments (Table 1) This may be due to the much lower S content of these samples (Table 1) generating lower concentrations of initial H_2O_2 combined with the basic pH of the solution (Fig. 5).

SSA is (strongly) correlated with H_2O_2 production in samples with non-acidic pH and similar S content, ($R^2 = 0.706$, Fig. 2c). It has been previously suggested that grain size (and thus SSA) is a primary control on the rate of pyrite oxidation (Rimstidt and Vaughan, 2003), and surface area has also been shown to play a key role on the kinetics of degradation of H_2O_2 by the Fenton reaction (Gil-Lozano et al., 2014).

4.2 Release of OC sources to the subglacial system

Microbes within subglacial environments are capable of recycling OM (e.g. Wadham et al. (2019), Lanoil et al. (2009), Priscu (2008), Christner et al. (2014), Skidmore (2011)), and concentrations above 0.08% (24 mM) H_2O_2 could inhibit these reactions by decreasing microbial populations (Medina-Cordoba et al., 2018) or by oxidising OM. Conversely, the generated H_2O_2 could have a net positive effect in these ecosystems by potentially re-activating legacy OM into more labile forms (Tranter, 2014). Previous crushing experiments found a significant increase in acetate between crushed and coarse sediment samples from Subglacial Lake Whillans which would provide a carbon source for both aerobic and anaerobic metabolisms, depending on redox conditions. All samples used in these experiments produced quantifiable concentrations of acetate (Fig. 4a), but only Ssv and JS samples showed statistically significant difference between crushed and coarse samples (Fig. 4a). There was no temporal trend or apparent correlation with H_2O_2 production, SSA or %OC content of samples (Supplementary A, Figure S1).

https://doi.org/10.5194/egusphere-2022-908
Preprint. Discussion started: 5 October 2022

It is worth noting that there are several methodological differences between these and previous studies, one of the most significant being the incubation time. These samples were only incubated for 25 hours, whilst previous studies which showed major differences in acetate production between crushed and coarse samples were conducted over 41 days (Gill-Olivas et al., 2021). Further, the current study was conducted at 4 °C, slightly higher than previous studies which were incubated at 0 °C. This temperature difference may have a minor effect on the rate of acetate production, with in situ rates closer to those at 0 °C.

There were no discernible temporal trends or correlations between formate and H_2O_2 production, SSA or %OC content of samples, but there was a noticeable increase in formate concentrations in crushed samples versus their uncrushed counterparts, even in these short incubations (Fig. 4b). There was no formate detected in previous incubations of crushed SLW samples (Gill-Olivas et al., 2021). Formate is a biologically significant compound, particularly in anaerobic environments where it has been shown to be utilised as an electron donor in a range of metabolisms (e.g. Madigan et al. (2020)).

The lack of a temporal trend in organic acid concentrations would suggest H_2O_2 did not affect the increase or decrease of organics. SSv had the highest OC content (Table 1), yet it had some of the lowest concentrations of acetate and formate in both crushed and coarse samples (Fig. 4). Conversely, JS and SLM samples, which produced much lower H_2O_2 concentrations, had much higher concentrations of these short chain, bio-available organics, despite having considerably lower %OC. Furthermore, the increase in formate between coarse and crushed samples was much more noticeable for these samples, where H_2O_2 concentrations were lower. These results could suggest that while abrasion may increase the production of bio-available OC in solutions, they may be oxidised when H_2O_2 concentrations are also generated.

4.3 Bio-available gases

Methanogens have been found in many subglacial systems, including Robertson Glacier (Boyd et al., 2010), SLW (Michaud et al., 2017), which is within the same broad hydrological system as SLM, both being fed by waters from Whillans Ice Stream (Carter et al., 2013), and glaciers on Svalbard (Stibal et al., 2012; Kaštovská et al., 2007). It is likely that subglacial methanogens are capable of hydrogenotrophy, utilising H_2 and CO_2 to generate CH_4 (Stibal et al., 2012). Thus, the release of H_2 in all samples, and of CO_2 from most samples, during crushing has the potential to stimulate methanogenic populations found in these environments. Further, there have been reports of methanotrophic organisms in certain subglacial environments (Michaud et al., 2017) which could utilise the CH_4 released by all crushed samples (Table 2).

Thermal degradation of OM during the formation of shales can generate H_2, CO_2 and CH_4 which can then be trapped within pore spaces of these and associated sedimentary rocks (Suzuki et al., 2017). Erosion of these sedimentary rocks opens interpore spaces and releases any gases trapped in them (Macdonald et al., 2018). The CH_4, C_2H_6 and CO_2 released by crushing RMC samples were within the range found in previous crushing studies using muddy carbonate rock samples from Robertson Glacier

https://doi.org/10.5194/egusphere-2022-908
Preprint. Discussion started: 5 October 2022

(Macdonald et al., 2018). Crushed RMC samples also continued to release CH_4 during their incubation suggesting wetting and mineral dissolution are important in this process (Fig. 6).

There are a few other mechanisms by which H_2 might be produced, both of which involve surface silica radicals (Si·) generated during erosion of these samples. One mechanism involves H_2 generation from the reaction of water with Si· (Eq. (R7) and (R8); e.g. Hasegawa et al. (1995), Kita et al. (1982), Telling et al. (2015)). The other mechanism is the potential reaction of hydroxyl functional groups (-OH) from within the crystal structure with Si·(Eq. (R18); Kameda et al. (2004)). This mechanism generates H·, which react together to generate H_2 (Eq. (R8)) from -OH rich minerals and clays (Kameda et al., 2004), and was suggested as a potential mechanism for H_2 generation when crushing of Robertson Glacier muddy carbonate samples (Macdonald et al., 2018).

$$\equiv \mathrm{Si}\cdot + \mathrm{AlOH} \rightarrow \equiv \mathrm{Si} - \mathrm{O} - \mathrm{Al} + \mathrm{H}\cdot \quad \text{(R18)}$$

4.4 Erosion as a source of ammonium for nitrifiers

Nitrification involves the sequential oxidation of NH_4^+ to NO_3^- (Eq. (R19) and (R20)).

$$NH_3 + O_2 \rightarrow NO_2^- + 3H^+ + 2e^- \quad \text{(R19)}$$

$$NO_2^- + H_2O \rightarrow NO_3 + 2H^+ + 2e^- \quad \text{(R20)}$$

There is evidence of nitrification in several subglacial systems, including Svalbard (Hodson et al., 2010; Wynn et al., 2007), Robertson Glacier (Boyd et al., 2011), and Subglacial Lake Whillans (Christner et al., 2014). Foght et al. (2004), suggested that the source of NH_4^+ to these environments is from *in situ* nitrogen fixation. However, incubations of subglacial sediments have been unsuccessful in detecting N- fixation despite the detection of nitrogen fixing bacteria (Boyd et al., 2011). Others have suggested exogenous sources of organic N to the system, such as wind-blown debris which was originally deposited on the glacier surface (Stibal et al., 2008). This debris is high in organic carbon, and so is likely to contain significant concentrations of organic N (Boyd et al., 2011). It is then washed into the subglacial system through moulins and crevasses (Boyd et al., 2011; Stibal et al., 2008), where it can then be mineralised and utilised for nitrification. Saros et al. (2010), reported that in catchments in the northern Rockies, lakes fed by snowpack and glacial meltwaters, often contained ten (and up to 200) times the amount of nitrate when compared to similar adjacent lakes fed only by snowpack meltwaters (SF lakes), implying processes such as nitrification occurred in the glaciated/glacial catchment. Crushing of sedimentary rocks from alpine catchments and incubation with water at higher temperatures (20°C) has shown release of ammonium (Montross et al., 2013a), similarly, from gneissic rocks from a glaciated catchment at (4°C) (Allen, 2019). Our results also indicate rock comminution can act as a source of NH_4^+ to the subglacial system. Crushing of glacial rock samples in the ball mill generates heat (Stone et al., 2022), which might have contributed to the NH_4^+ measured. However, there was no correlation between NH_4^+ and %N or

https://doi.org/10.5194/egusphere-2022-908
Preprint. Discussion started: 5 October 2022

%OC in the samples. Most likely, NH_4^+ in solution is a direct result of the release of NH_4^+ from clay minerals (Boyd, 1997) or from silicate mineral surfaces (Sugahara et al., 2017).

No matter the source, it is clear that abrasion increases the availability of NH_4^+ for nitrification. Crude calculations can be made to estimate the potential NH_4^+ generated from abrasion at a catchment level using suspended sediment fluxes. We estimate that Robertson Glacier (for RMC) and Longyearbreen (for SSv) could generate 3.5 and 4.7 µmol NH_4^+ m^{-2} day^{-1}, respectively (Supplementary B). Incubations of subglacial samples from Robertson Glacier suggest that nitrifiers utilised 0.2 µmol NH_4^+ m^{-2} day^{-1} (Supplementary B; Boyd et al. (2011)), at peak activity, yet no nitrogen fixers were found. Therefore, subglacial abrasion could be a key source of NH_4^+ to these ecosystems. This finding would be consistent with recent research that showed bedrock N inputs from weathering are of a similar magnitude to atmospheric inputs in many terrestrial environments (Houlton et al., 2018). Further, in the presence of catalase, H_2O_2 dissociates into O_2 and H_2O. Thus, H_2O_2 can be a source of dissolved oxygen which improves nitrification in systems with limited O_2, such as wetlands (Dinakar et al., 2020), and could theoretically aid nitrification in subglacial systems.

5 Conclusions

It is often difficult to disentangle the many confounding factors when trying to understand the interactions of competing processes in natural systems. Subglacial environments are no exception. We anticipated that the concentration of sulphide in sedimentary rocks would have a first order impact on the amount of H_2O_2 that is generated when the rocks are crushed. Instead, we found that the presence or concentration of pyrite is not enough to predict the generation of H_2O_2 from abrasion. Our results suggest that the presence of carbonates and the pH of the solution will impact the concentrations of H_2O_2 generated. Other factors, such as SSA, will influence H_2O_2 generation at similar pH. This study suggests that erosion can provide sources of nutrients and energy (including CH_4, H_2, labile forms of OC in the forms of VFA's and NH_4^+) to subglacial ecosystems. Caution should be taken to avoid over-extrapolation of these results as these experiments use only a limited range of subglacial sedimentary samples. However, these results serve to highlight the potential role that abrasion plays in sustaining subglacial sedimentary rock-hosted aquatic ecosystems.

Data Availability

All data presented in Figs. 1 - 6 are available online (Data Repository Link to be updated).

https://doi.org/10.5194/egusphere-2022-908
Preprint. Discussion started: 5 October 2022

Supplement Link

Author Contributions:

BGO led the design of the study, assisted by MT and JT. Experimental work and laboratory analysis was performed by BGO. BGO prepared this manuscript with contributions from MT, JT and MS.

Competing Interests

The authors declare that they have no conflict of interest.

Acknowledgements

The research was supported by NERC grant NE/S001670/1, CRUSH2LIFE (BGO, MT, JT) and NSF-OPP 1543537 (MS). Moya MacDonald provided siltstone samples from Svalbard (SSv)

References

Allen, J. J.: Glacial effects on stream water nitrate: an examination of paired catchments in southern Montana., Earth Sciences, Montana State University, 2019.

Anderson, S. P.: Glaciers show direct linkage between erosion rate and chemical weathering fluxes, Geomorphology, 67, 147-157, 10.1016/j.geomorph.2004.07.010, 2005.

Baga, A. N., Johnson, G. R. A., Nazhat, N. B., and Saadalla-Nazhat, R. A.: A simple spectrophotometric determination of hydrogen peroxide at low concentrations in aqueous solution, Analytica Chimica Acta, 204, 349-353, 10.1016/S0003-2670(00)86374-6, 1988.

Bak, E. N., Zafirov, K., Merrison, J. P., Jensen, S. J. K., Nornberg, P., Gunnlaugsson, H. P., and Finster, K.: Production of reactive oxygen species from abraded silicates. Implications for the reactivity of the Martian soil, Earth and Planetary Science Letters, 473, 113-121, 10.1016/j.epsl.2017.06.008, 2017.

Bataineh, H., Pestovsky, O., and Bakac, A.: pH-induced mechanistic changeover from hydroxyl radicals to iron(iv) in the Fenton reaction, Chemical Science, 3, 1594-1599, 10.1039/C2SC20099F, 2012.

Borda, M. J., Elsetinow, A. R., Schoonen, M. A., and Strongin, D. R.: Pyrite-Induced Hydrogen Peroxide Formation as a Driving Force in the Evolution of Photosynthetic Organisms on an Early Earth, Astrobiology, 1, 283-288, 10.1089/15311070152757474, 2001.

Borda, M. J., Elsetinow, A. R., Strongin, D. R., and Schoonen, M. A.: A mechanism for the production of hydroxyl radical at surface defect sites on pyrite, Geochimica et Cosmochimica Acta, 67, 935-939, 10.1016/S0016-7037(02)01222-X, 2003.

Boyd, E. S., Skidmore, M., Mitchell, A. C., Bakermans, C., and Peters, J. W.: Methanogenesis in subglacial sediments, Environmental Microbiology Reports, 2, 685-692, 10.1111/j.1758-2229.2010.00162.x, 2010.

Boyd, E. S., Lange, R. K., Mitchell, A. C., Havig, J. R., Hamilton, T. L., Lafrenière, M. J., Shock, E. L., Peters, J. W., and Skidmore, M.: Diversity, Abundance, and Potential Activity of Nitrifying and Nitrate-Reducing Microbial Assemblages in a Subglacial Ecosystem, 77, 4778-4787, 10.1128/AEM.00376-11, 2011.

Boyd, S. R.: Determination of the ammonium content of potassic rocks and minerals by capacitance manometry: a prelude to the calibration of FTIR microscopes, Chemical Geology, 137, 57-66, 10.1016/S0009-2541(96)00150-7, 1997.

Campbell, T., Patterson, M. O., Skidmore, M. L., Leventer, A., Michaud, A. B., Rosenheim, B. E., Harwood, D. M., Dore, J. E., Tranter, M., Venturelli, R., and Priscu, J. C.: Physical and chemical characterization of sediments from Mercer Subglacial Lake, West Antarctica, December 01, 20192019.

Carter, S. P., Fricker, H. A., and Siegfried, M. R.: Evidence of rapid subglacial water piracy under Whillans Ice Stream, West Antarctica, Journal of Glaciology, 59, 1147-1162, 10.3189/2013JoG13J085, 2013.

https://doi.org/10.5194/egusphere-2022-908
Preprint. Discussion started: 5 October 2022

Christner, B. C., Priscu, J. C., Achberger, A. M., Barbante, C., Carter, S. P., Christianson, K., Michaud, A. B., Mikucki, J. A., Mitchell, A. C., Skidmore, M. L., Vick-Majors, T. J., and Team, W. S.: A microbial ecosystem beneath the West Antarctic ice sheet, Nature, 512, 310-+, 10.1038/nature13667, 2014.

Dinakar, M., Tao, W., and Daley, D.: Using hydrogen peroxide to supplement oxygen for nitrogen removal in constructed wetlands, Journal of Environmental Chemical Engineering, 8, 104517, 10.1016/j.jece.2020.104517, 2020.

Dunham, E. C., Dore, J. E., Skidmore, M. L., Roden, E. E., and Boyd, E. S.: Lithogenic hydrogen supports microbial primary production in subglacial and proglacial environments, 118, e2007051117, 10.1073/pnas.2007051117 %J Proceedings of the National Academy of Sciences, 2021.

Edgar, J. O., Gilmour, K., White, M. L., Abbott, G. D., and Telling, J.: Aeolian driven oxidant and hydrogen generation in Martian regolith: The role of mineralogy and abrasion temperature, Earth and Planetary Science Letters, 579, 117361, 10.1016/j.epsl.2021.117361, 2022.

Elvevold, S., Dallmann, W., and Blomeier, D.: Geology of Svalbard, Norwegian Polar Institute/ Norsk Polarinstitutt, Tromsø (Norway), 2007.

Foght, J., Aislabie, J., Turner, S., Brown, C. E., Ryburn, J., Saul, D. J., and Lawson, W.: Culturable bacteria in subglacial sediments and ice from two Southern Hemisphere glaciers, Microbial Ecology, 47, 329-340, 10.1007/s00248-003-1036-5, 2004.

Folk, R. L. and Ward, W. C.: Brazos River bar [Texas]; a study in the significance of grain size parameters, Journal of Sedimentary Research, 27, 3-26, 10.1306/74d70646-2b21-11d7-8648000102c1865d, 1957.

Gil-Lozano, C., Losa-Adams, E., Davila, A. F., and Gago-Duport, L.: Pyrite nanoparticles as a Fenton-like reagent for in situ remediation of organic pollutants, Beilstein Journal of Nanotechnology, 5, 855-864, 10.3762/bjnano.5.97, 2014.

Gil-Lozano, C., Davila, A. F., Losa-Adams, E., Fairén, A. G., and Gago-Duport, L.: Quantifying Fenton reaction pathways driven by self-generated H2O2 on pyrite surfaces, Scientific Reports, 7, 43703, 10.1038/srep43703, 2017.

Gill-Olivas, B., Telling, J., Tranter, M., Skidmore, M., Christner, B., O'Doherty, S., and Priscu, J.: Subglacial erosion has the potential to sustain microbial processes in Subglacial Lake Whillans, Antarctica, Communications Earth & Environment, 2, 134, 10.1038/s43247-021-00202-x, 2021.

Harris, D., Horwáth, W. R., and van Kessel, C.: Acid fumigation of soils to remove carbonates prior to total organic carbon or CARBON-13 isotopic analysis, Soil Science Society of America Journal, 65, 1853-1856, 10.2136/sssaj2001.1853, 2001.

Hasegawa, M., Ogata, T., and Sato, M.: Mechano-radicals produced from ground quartz and quartz glass, Powder Technology, 85, 269-274, 10.1016/0032-5910(96)80150-1, 1995.

He, H., Wu, X., Xian, H., Zhu, J., Yang, Y., Lv, Y., Li, Y., and Konhauser, K. O.: An abiotic source of Archean hydrogen peroxide and oxygen that pre-dates oxygenic photosynthesis, Nature Communications, 12, 6611, 10.1038/s41467-021-26916-2, 2021.

Hodson, A., Tranter, M., and Vatne, G.: Contemporary rates of chemical denudation and atmospheric CO2 sequestration in glacier basins: An Arctic perspective, Earth Surface Processes and Landforms, 25, 1447-1471, 10.1002/1096-9837(200012)25:13<1447::aid-esp156>3.0.co;2-9, 2000.

Hodson, A., Roberts, T. J., Engvall, A.-C., Holmén, K., and Mumford, P.: Glacier ecosystem response to episodic nitrogen enrichment in Svalbard, European High Arctic, Biogeochemistry, 98, 171-184, 10.1007/s10533-009-9384-y, 2010.

Hodson, A., Anesio, A. M., Tranter, M., Fountain, A., Osborn, M., Priscu, J., Laybourn-Parry, J., and Sattler, B.: Glacial ecosystems, Ecological Monographs, 78, 41-67, 10.1890/07-0187.1, 2008.

Hodson, T. O., Powell, R. D., Brachfeld, S. A., Tulaczyk, S., Scherer, R. P., and Team, W. S.: Physical processes in Subglacial Lake Whillans, West Antarctica: Inferences from sediment cores, Earth and Planetary Science Letters, 444, 56-63, 10.1016/j.epsl.2016.03.036, 2016.

Hood, E., Fellman, J., Spencer, R. G. M., Hernes, P. J., Edwards, R., D'Amore, D., and Scott, D.: Glaciers as a source of ancient and labile organic matter to the marine environment, Nature, 462, 1044-1047, 10.1038/nature08580, 2009.

Houlton, B. Z., Morford, S. L., and Dahlgren, R. A.: Convergent evidence for widespread rock nitrogen sources in Earth’s surface environment, Science, 360, 58-62, doi:10.1126/science.aan4399, 2018.

Illes, E., Mizrahi, A., Marks, V., and Meyerstein, D.: Carbonate-radical-anions, and not hydroxyl radicals, are the products of the Fenton reaction in neutral solutions containing bicarbonate, Free Radical Biology and Medicine, 131, 1-6, 10.1016/j.freeradbiomed.2018.11.015, 2019.

Kameda, J., Saruwatari, K., and Tanaka, H.: H-2 generation during dry grinding of kaolinite, Journal of Colloid and Interface Science, 275, 225-228, 10.1016/j.jcis.2004.02.014, 2004.

Kaštovská, K., Stibal, M., Šabacká, M., Černá, B., Šantrůčková, H., and Elster, J.: Microbial community structure and ecology of subglacial sediments in two polythermal Svalbard glaciers characterized by epifluorescence microscopy and PLFA, Polar Biology, 30, 277-287, 10.1007/s00300-006-0181-y, 2007.

Kita, I., Matsuo, S., and Wakita, H.: H2 generation by reaction between H2O and crushed rock - An experimental-study on H2 degassing from the active fault zone, Journal of Geophysical Research, 87, 789-795, 10.1029/JB087iB13p10789, 1982.

Kohler, T. J., Žárský, J. D., Yde, J. C., Lamarche-Gagnon, G., Hawkings, J. R., Tedstone, A. J., Wadham, J. L., Box, J. E., Beaton, A. D., and Stibal, M.: Carbon dating reveals a seasonal progression in the source of particulate organic carbon exported from the Greenland Ice Sheet, 44, 6209-6217, 10.1002/2017GL073219, 2017.

https://doi.org/10.5194/egusphere-2022-908
Preprint. Discussion started: 5 October 2022

Lanoil, B., Skidmore, M., Priscu, J. C., Han, S., Foo, W., Vogel, S. W., Tulaczyk, S., and Engelhardt, H.: Bacteria beneath the West Antarctic Ice Sheet, Environmental Microbiology, 11, 609-615, 10.1111/j.1462-2920.2008.01831.x, 2009.
Lawson, E. C., Wadham, J. L., Tranter, M., Stibal, M., Lis, G. P., Butler, C. E. H., Laybourn-Parry, J., Nienow, P., Chandler, D., and Dewsbury, P.: Greenland Ice Sheet exports labile organic carbon to the Arctic oceans, Biogeosciences, 11, 4015-4028, 10.5194/bg-11-4015-2014, 2014.
Le, P. T. T. and Boyd, C. E.: Comparison of Phenate and Salicylate Methods for Determination of Total Ammonia Nitrogen in Freshwater and Saline Water, Journal of the World Aquaculture Society, 43, 885-889, 10.1111/j.1749-7345.2012.00616.x, 2012.
Lerman, A.: Dissolution of Feldspars, in: Geochemical Processes Water and Sediment Environments, Robert E. Krieager Publishing Company, Malabar, florida, 244 -248, 1988.
Macdonald, M. L., Wadham, J. L., Telling, J., and Skidmore, M. L.: Glacial Erosion Liberates Lithologic Energy Sources for Microbes and Acidity for Chemical Weathering Beneath Glaciers and Ice Sheets, Front. Earth Sci., 6, 15, 10.3389/feart.2018.00212, 2018.
Madigan, M. T., Bender, K. S., Buckley, D. H., Sattley, W. M., and Stahl, D. A.: Brock Biology of Microorganisms, 16th edition, Pearson2020.
McMechan, M. E.: Geology, Peter Lougheed Provincial Park, west of fifth meridian, Alberta, Geological Survey of Canada, "A" Series Map 1920A, 10.4095/209966, 1998.
Medina-Cordoba, L. K., Valencia-Mosquera, L. L., Tarazona-Diaz, G. P., and Arias-Palacios, J. D. C.: Evaluation of the efficacy of a hydrogen peroxide disinfectant, International Journal of Pharmacy and Pharmaceutical Sciences, 10, 104-108, 10.22159/ijpps.2018v10i10.24652, 2018.
Michaud, A. B., Dore, J. E., Achberger, A. M., Christner, B. C., Mitchell, A. C., Skidmore, M. L., Vick-Majors, T. J., and Priscu, J. C.: Microbial oxidation as a methane sink beneath the West Antarctic Ice Sheet, Nature Geoscience, 10, 582-+, 10.1038/ngeo2992, 2017.
Michaud, A. B., Skidmore, M. L., Mitchell, A. C., Vick-Majors, T. J., Barbante, C., Turetta, C., vanGelder, W., and Priscu, J. C.: Solute sources and geochemical processes in Subglacial Lake Whillans, West Antarctica, Geology, 44, 347-350, 10.1130/g37639.1, 2016.
Montross, G. G., McGlynn, B. L., Montross, S. N., and Gardner, K. K.: Nitrogen production from geochemical weathering of rocks in southwest Montana, USA, Journal of Geophysical Research-Biogeosciences, 118, 1068-1078, 10.1002/jgrg.20085, 2013a.
Montross, S. N., Skidmore, M., Tranter, M., Kivimäki, A.-L., and Parkes, R. J.: A microbial driver of chemical weathering in glaciated systems, Geology, 41, 215-218, 10.1130/G33572.1 %J Geology, 2013b.
Nesbitt, H. W., Bancroft, G. M., Pratt, A. R., and Scaini, M. J.: Sulfur and iron surface states on fractured pyrite surfaces %J American Mineralogist, 83, 1067-1076, doi:10.2138/am-1998-9-1015, 1998.
Plummer, L. N., Wigley, T. M., and Parkhurst, D. L.: The kinetics of calcite dissolution in CO 2 -water systems at 5 degrees to 60 ºC and 0.0 to 1.0 atm CO_2., American Journal of Chemistry, 278, 179 - 216, 1978.
Priscu, J. C., Kalin, J., Winans, J., Campbell, T., Siegfried, M. R., Skidmore, M., Dore, J. E., Leventer, A., Harwood, D. M., Duling, D., Zook, R., Burnett, J., Gibson, D., Krula, E., Mironov, A., McManis, J., Roberts, G., Rosenheim, B. E., Christner, B. C., Kasic, K., Fricker, H. A., Lyons, W. B., Barker, J., Bowling, M., Collins, B., Davis, C., Gagnon, A., Gardner, C., Gustafson, C., Kim, O.-S., Li, W., Michaud, A., Patterson, M. O., Tranter, M., Venturelli, R., Vick-Majors, T., and Elsworth, C.: Scientific access into Mercer Subglacial Lake: scientific objectives, drilling operations and initial observations, Ann. Glaciol., 62, 340-352, 10.1017/aog.2021.10, 2021.
Priscu, J. C., Tulaczyk, S., Studinger, M., Kennicutt, M.C., II, Christner, B., and Foreman, C. : Antarctic subglacial water: origin, evolution, and ecology, in: Polar Lakes and Rivers, edited by: Vincent, W. F. a. L.-P., J., Oxford University Press, Oxford, UK, 119-136, 2008.
Rimstidt, J. D. and Vaughan, D. J.: Pyrite oxidation: a state-of-the-art assessment of the reaction mechanism, Geochimica et Cosmochimica Acta, 67, 873-880, 10.1016/S0016-7037(02)01165-1, 2003.
Saros, J. E., Rose, K. C., Clow, D. W., Stephens, V. C., Nurse, A. B., Arnett, H. A., Stone, J. R., Williamson, C. E., and Wolfe, A. P.: Melting Alpine Glaciers Enrich High-Elevation Lakes with Reactive Nitrogen, Environmental Science & Technology, 44, 4891-4896, 10.1021/es100147j, 2010.
Saruwatari, K., Kameda, J., and Tanaka, H.: Generation of hydrogen ions and hydrogen gas in quartz-water crushing experiments: an example of chemical processes in active faults, Physics and Chemistry of Minerals, 31, 176-182, 10.1007/s00269-004-0382-2, 2004.
Skidmore, M.: Microbial communities in Antarctic subglacial aquatic environments, Washington DC American Geophysical Union Geophysical Monograph Series, 192, 61-81, 2011.
Skidmore, M., Tranter, M., Tulaczyk, S., and Lanoil, B.: Hydrochemistry of ice stream beds - evaporitic or microbial effects?, Hydrological Processes, 24, 517-523, 10.1002/hyp.7580, 2010.
Souchez, R., Jouzel, J., Landais, A., Chappellaz, J., Lorrain, R., and Tison, J.-L.: Gas isotopes in ice reveal a vegetated central Greenland during ice sheet invasion, 33, 10.1029/2006GL028424, 2006.
Stibal, M., Tranter, M., Benning, L. G., and Řehák, J.: Microbial primary production on an Arctic glacier is insignificant in comparison with allochthonous organic carbon input, 10, 2172-2178, 10.1111/j.1462-2920.2008.01620.x, 2008.
Stibal, M., Wadham, J. L., Lis, G. P., Telling, J., Pancost, R. D., Dubnick, A., Sharp, M. J., Lawson, E. C., Butler, C. E. H., Hasan, F., Tranter, M., and Anesio, A. M.: Methanogenic potential of Arctic and Antarctic subglacial environments with contrasting organic carbon sources, Global Change Biology, 18, 3332-3345, 10.1111/j.1365-2486.2012.02763.x, 2012.

https://doi.org/10.5194/egusphere-2022-908
Preprint. Discussion started: 5 October 2022

Stillings, M., Lunn, R. J., Pytharouli, S., Shipton, Z. K., Kinali, M., Lord, R., and Thompson, S.: Microseismic Events Cause Significant pH Drops in Groundwater, 48, e2020GL089885, 10.1029/2020GL089885, 2021.
Stone, J., Edgar, J. O., Gould, J. A., and Telling, J.: Tectonically-driven oxidant production in the hot biosphere, Nature Communications, 13, 4529, 10.1038/s41467-022-32129-y, 2022.
Sugahara, H., Takano, Y., Ogawa, N. O., Chikaraishi, Y., and Ohkouchi, N.: Nitrogen Isotopic Fractionation in Ammonia during Adsorption on Silicate Surfaces, ACS Earth and Space Chemistry, 1, 24-29, 10.1021/acsearthspacechem.6b00006, 2017.
Suzuki, N., Saito, H., and Hoshino, T.: Hydrogen gas of organic origin in shales and metapelites, International Journal of Coal Geology, 173, 227-236, 10.1016/j.coal.2017.02.014, 2017.
Takehiro, H., Shinsuke, K., and Katsuhiko, S.: Mechanoradical H2 generation during simulated faulting: Implications for an earthquake-driven subsurface biosphere, Geophysical Research Letters, 38, 10.1029/2011GL048850, 2011.
Telling, J., Boyd, E. S., Bone, N., Jones, E. L., Tranter, M., MacFarlane, J. W., Martin, P. G., Wadham, J. L., Lamarche-Gagnon, G., Skidmore, M. L., Hamilton, T. L., Hill, E., Jackson, M., and Hodgson, D. A.: Rock comminution as a source of hydrogen for subglacial ecosystems, Nature Geosci, 8, 851-855, 10.1038/ngeo2533, 2015.
Tranter, M.: Geochemical Weathering in Glacial and Proglacial Environments., in: Treatise on Geochemistry, edited by: Holland, H. D., and Turekian, K. K., Elsevier-Permagon, Oxford, 189 - 205, 10.1016/B0-08-043751-6/05078-7, 2003.
Tranter, M.: BIOGEOCHEMISTRY Microbes eat rock under ice, Nature, 512, 256-257, 10.1038/512256a, 2014.
Tranter, M.: Grand challenge for low temperature and pressure geochemistry—sparks in the dark, on Earth, Mars, and throughout the Galaxy, 3, 10.3389/feart.2015.00069, 2015.
Tranter, M., Skidmore, M., and Wadham, J.: Hydrological controls on microbial communities in subglacial environments, Hydrological Processes, 19, 995-998, 10.1002/hyp.5854, 2005.
Tranter, M., Brown, G., Raiswell, R., Sharp, M., and Gurnell, A.: A conceptual model of solute acquisition by Alpine glacial meltwaters, Journal of Glaciology, 39, 573-581, 10.3189/S0022143000016464, 1993.
Tranter, M., Sharp, M. J., Lamb, H. R., Brown, G. H., Hubbard, B. P., and Willis, I. C.: Geochemical weathering at the bed of Haut Glacier d'Arolla, Switzerland - a new model, Hydrological Processes, 16, 959-993, 10.1002/hyp.309, 2002a.
Tranter, M., Huybrechts, P., Munhoven, G., Sharp, M. J., Brown, G. H., Jones, I. W., Hodson, A. J., Hodgkins, R., and Wadham, J. L.: Direct effect of ice sheets on terrestrial bicarbonate, sulphate and base cation fluxes during the last glacial cycle: minimal impact on atmospheric CO2 concentrations, Chemical Geology, 190, 33-44, 10.1016/s0009-2541(02)00109-2, 2002b.
Tulaczyk, S., Kamb, B., Scherer, R. P., and Engelhardt, H. F.: Sedimentary processes at the base of a West Antarctic ice stream: Constraints from textural and compositional properties of subglacial debris, Journal of Sedimentary Research, 68, 487-496, 1998.
Viollier, E., Inglett, P. W., Hunter, K., Roychoudhury, A. N., and Van Cappellen, P.: The ferrozine method revisited: Fe(II)/Fe(III) determination in natural waters, Applied Geochemistry, 15, 785-790, 10.1016/s0883-2927(99)00097-9, 2000.
Wadham, J. L., Hawkings, J. R., Tarasov, L., Gregoire, L. J., Spencer, R. G. M., Gutjahr, M., Ridgwell, A., and Kohfeld, K. E.: Ice sheets matter for the global carbon cycle, Nature Communications, 10, 3567, 10.1038/s41467-019-11394-4, 2019.
Wadham, J. L., Tranter, M., Skidmore, M., Hodson, A. J., Priscu, J., Lyons, W. B., Sharp, M., Wynn, P., and Jackson, M.: Biogeochemical weathering under ice: Size matters, Global Biogeochemical Cycles, 24, 11, 10.1029/2009gb003688, 2010.
Wakita, H., Nakamura, Y., Kita, I., Fujii, N., and Notsu, K.: Hydrogen release - New indicator of fault activity., Science, 210, 188-190, 10.1126/science.210.4466.188, 1980.
Wiebe, R. and Gaddy, V. L.: The Solubility of Hydrogen in Water at 0, 50, 75 and 100° from 25 to 1000 Atmospheres, Journal of the American Chemical Society, 56, 76-79, 10.1021/ja01316a022, 1934.
Wynn, P. M., Hodson, A. J., Heaton, T. H. E., and Chenery, S. R.: Nitrate production beneath a High Arctic glacier, Svalbard, Chemical Geology, 244, 88-102, 10.1016/j.chemgeo.2007.06.008, 2007.
Zhou, S., Zhang, D., Wang, H., and Li, X.: A modified BET equation to investigate supercritical methane adsorption mechanisms in shale, Marine and Petroleum Geology, 105, 284-292, 10.1016/j.marpetgeo.2019.04.036, 2019.